Cyclin-dependent kinase 12, a novel drug target for visceral leishmaniasis

Authors: Susan Wyllie[a], Michael Thomas[a], Stephen Patterson[a], Sabrinia Crouch[b], Manu De Rycker[a], Rhiannon Lowe[c], Stephanie Gresham[c], Michael Urbaniak[a,d], Thomas Otto[e], Laste Stojanovski[a], Frederick Simeons[a], Sujatha Manthri[a], Lorna M. MacLean[a], Fabio Zuccotto[a], Nadine Homeyer[a], Hannah Pflaumer[f], Markus Boesche[f], Lalitha Sastry[a], Paul Connolly[g], Sebastian Albrecht[a], Matt Berriman[e], Gerard Drewes[f], David W. Gray[a], Sonja Ghidelli-Disse[f], Susan Dixon[h], Jose M. Fiandor[b], Paul G. Wyatt[a], Michael A. J. Ferguson[a], Alan H. Fairlamb[a], Timothy J. Miles[b*], Kevin D. Read[a*], Ian H. Gilbert[a*]

Affiliations:

[a] Drug Discovery Unit, Division of Biological Chemistry and Drug Discovery, School of Life Sciences, University of Dundee, Dundee, United Kingdom.

[b] Diseases of the Developing World, GlaxoSmithKline, Calle Severo Ochoa 2, 28760, Tres Cantos, Madrid, Spain

[c] GlaxoSmithKline, David Jack Centre for R&D, Park Road, Ware, Hertfordshire, SG12 0DP, UK

[d] Division of Biomedical and Life Sciences, Faculty of Health and Medicine, Lancaster University, Lancaster LA1 4YG, UK

[e] Wellcome Trust Sanger Institute, Hinxton, Cambridge CB10 1SA, UK.

[f] Cellzome - a GlaxoSmithKline company, Meyerhofstrasse 1 69117 Heidelberg, Germany

[g] GlaxoSmithKline, New Frontiers Science Park, Third Avenue, Harlow, Essex. CM19 5AW, UK.

[h] GlaxoSmithKline, Stockley Park West, West Drayton, Uxbridge, UB11 1BT, UK

Summary

Visceral leishmaniasis (VL) causes significant mortality and morbidity in many parts of the world. There is an urgent need for the development of new, effective treatments for this disease. We describe the development of a novel anti-leishmanial drug-like chemical series based on a pyrazolopyrimidine scaffold. The leading compound from this series (**5, DDD853651/ GSK3186899**) is efficacious in a mouse model of visceral leishmaniasis and has suitable physicochemical, pharmacokinetic and toxicological properties for further development and has been declared a preclinical candidate. Detailed mode of action studies indicate that compounds from this series act principally by inhibiting the parasite cdc-2-related kinase 12 (CRK12), thus defining a novel, druggable, target for visceral leishmaniasis.

Introduction:

Leishmania parasites cause a wide spectrum of human infections ranging from the life-threatening visceral disease to disfiguring mucosal and cutaneous forms. *Leishmania* spp. are obligate intracellular parasites of the vertebrate reticuloendothelial system, where they multiply as amastigotes within macrophage phagolysosomes; transmission is by blood-sucking sandflies, in which they proliferate as extracellular promastigotes.

Visceral leishmaniasis (VL), resulting from infection with *Leishmania donovani* and *L. infantum*, causes more than 30,000 deaths annually, of which ~60% occur in India, Bangladesh and Nepal[1]. In 95% of cases, death can be prevented by timely and appropriate drug therapy[2]. However, current treatment options are far from ideal with outcomes dependent upon a number of factors including geographical location, the immune status and other co-morbidities of the patient, and the disease classification. None of the current front-line treatments for VL, Ambisome, miltefosine, paromomycin and antimonials, are ideal for use in resource poor settings, due to issues

such as teratogenicity, cost, resistance and / or clinical relapse, prolonged treatment regimens and parenteral administration[3-5]. Thus, there is an urgent need for new treatment options for VL, particularly oral drugs. Unfortunately, there are currently no new therapeutics in clinical development and few in preclinical development. Drug discovery efforts have been hampered by a paucity of well-validated molecular drug targets in *Leishmania,* while whole cell (phenotypic) screening programs have been hindered by extremely low hit rates [6]. Here, we report the discovery of an exciting new anti-leishmanial compound with a novel mechanism of action.

Discovery

Recently, we reported the identification of a diaminothiazole series from a compound screen against *Trypanosoma brucei* GSK3 kinase (*Tb*GSK3)[7]. During compound optimization it became clear that the anti-trypanosomal activity of the series was driven, at least in part, by off-target activity. The diaminothiazoles were active against *T. brucei* bloodstream trypanosomes in viability assays, but were essentially inactive against *L. donovani* axenic amastigotes. Modification of the core structure, whilst retaining hydrogen bond donor and acceptor functionalities, gave a bicyclic compound series (Fig. 1), one of which (compound **2)**, showed very weak activity against *L. donovani* axenic amastigotes, but was inactive against the pharmacologically relevant intra-macrophage amastigotes. However this scaffold was amenable to optimization. Appending a sulfonamide to the cyclohexyl ring resulted in compound **3** which was active against *L. donovani* amastigotes in both the axenic and intra-macrophage assays[8] and selectively active against *L. donovani* compared to the THP-1 mammalian host cells used in the assay. Modification of the substituent on the pyrazole ring resulted in compound **4** which demonstrated >70% parasite reduction in a mouse model of VL when dosed orally.

Subsequent optimization of the series led to the discovery of the key compound **DDD853651 / GSK3186899** (compound **5**)[9], which is our preclinical compound. Compound **5** was active against *L. donovani* in an intra-macrophage assay[8] with an EC_{50} of 1.4 μM (95% CI 1.2-1.5 μM, n=12) and good selectivity against mammalian THP-1 cells (EC_{50} >50 μM). The compound was also active and cytocidal in our cidal axenic amastigote study (EC_{50} 0.1 μM (95% CI 0.06-0.17 μM, n=4)[10]. At a concentration of 0.2 μM, compound **5** was cytocidal at 96 h; increasing the concentration to 1.8 μM reduced this to 48 h (Extended Data Fig. S1). Screening compound **5** against a panel of *Leishmania* clinical isolates demonstrated a less than 10-fold variation in potency across different strains. The compound was also more active in a panel of leishmanial strains using human peripheral mononuclear cells as host cells (Extended Data Table 1).

Good solubility in relevant physiological media proved key for development of this series; compound solubility in Fasted State Simulated Intestinal Fluid (FaSSIF solubility) was used to drive the optimization (Extended Data Table 2). Compound **5** was stable in microsomes and hepatocytes, predictive of good metabolic stability (Extended Data Table 3). The compound was orally bioavailable and showed a linearity of pharmacokinetics from 10 to 300 mg/kg in rats (Extended Data Table 4). In a mouse model of VL infection the compound demonstrated comparable activity to the front-line anti-leishmanial drug miltefosine, reducing parasite levels by 99% when dosed orally twice a day for 10 days at 25 mg/kg (Extended Data Table 5).

The non-clinical safety data for compound **5** suggests a suitable therapeutic window for progression into regulatory preclinical studies. *In vitro* assays demonstrated that this compound did not significantly inhibit cytochrome P450 enzymes, which can lead to problematic drug-drug

interactions that are particularly relevant due to the frequency of VL/HIV co-infections[1]. As the series was developed from a known protein kinase scaffold[11,12], Cellzome's kinobead™ technology was used to determine if compound **5** potentially inhibits human protein kinases[13]. These experiments indicated that compound **5** interacted with four human kinases, MAPK11, NLK, MAPK14 and CDK7, at concentrations within multiples of the predicted clinical dose (**Table S1**). However, the extent of inhibition of these human kinases is not sufficient to preclude clinical development of the molecule and no significant inhibition of other human kinases was detected in the Kinobeads™ assays. Preclinical assessment of cardiovascular effects and genotoxicity did not reveal any issues that would prevent further development. Additionally, there were no significant adverse effects in a rat 7-day repeat dose oral toxicity study with respect to clinical chemistry and histopathology. Both the *in vivo* efficacy and safety profile of compound **5** support progression to definitive safety studies.

Mode of Action Studies

Elucidating the mode of action of novel chemical series can greatly benefit drug discovery campaigns[14]. Since there is no blueprint to establish the mode of action of bioactive small molecules[15,16], several complementary methodologies were employed using representative pyrazolopyrimidine analogues from the drug discovery program as chemical tools (Fig. 2a). These compounds showed very good activity correlation between the intra-macrophage, axenic amastigote and promastigote assays, which gave us confidence to use the extracellular parasite forms for mode of action studies where it was not possible to use the intracellular forms (**Table S2**).

As a first step towards identifying the target(s) of the leishmanocidal pyrazolopyrimidine series, a derivative was prepared with a polyethyleneglycol (PEG) linker (**9**; Fig. 2b) and covalently attached to magnetic beads to allow for chemical proteomics. Two methods were used. Firstly, the beads were used to pull down proteins from SILAC (Stable Isotope Labelling by Amino Acids in Cell Culture) labelled *L. donovani* promastigote lysates[17] in the presence ("light-labelled lysate") or absence ("heavy-labelled lysate") of 10 μM compound **10**, a structurally related, bioactive derivative of compound **9** (Fig. 2)[18]. After combining the bead eluates and performing proteomic analyses, proteins that bound specifically to the pyrazolopyrimidine pharmacophore could be distinguished from proteins that bound non-specifically to the beads by virtue of high heavy : light tryptic peptide isotope ratios. These experiments identified CRK12, CRK6, CYC9, CRK3, MAPK9, CYC6 and STE11 as specific binders to the compound **9**-derivatised beads (Log_2 heavy : light ratio >2.8; 7-fold enrichment) (Fig. S5; Table S3). In a second experiment, pull down experiments were conducted with beads derivatized with **9**, **11** or **12**, followed by competition studies with **7**, **6** and **6**, respectively. Adherent proteins were washed off the beads, digested with trypsin and labelled with isobaric tandem mass tags. Comparison of the labelled peptides derived from experiments with and without competition by liquid chromatography/ mass spectrometry identified proteins likely to specifically bind to the immobilized ligands. Potential candidates identified included: CRK3, CRK6, CRK12 CYC3, CYC6, CYC9, MAPK9, MAPK5 and several hypothetical proteins (Fig. S6; Table S4). Although such binding could be direct or indirect as part of a protein complex, these results are consistent with previous studies which report that the pyrazolopyrimidine core binds to protein kinases[11,19-21]. One of these binding kinases MAPK9 was not considered further as it is not expressed in the disease-relevant *Leishmania* amastigotes life-

cycle stage[22]. We also investigated immobilizing the compound at an alternate position on the scaffold and this gave a similar profile (Fig. S6), further validating the approach.

The presence of three cyclin related kinases (CRK3, 6 and 12) and three cyclins (CYC3, 6 and 9) in the initial target list led us to analyze the effects of four pyrazolopyrimidines (**6**, **7**, **8** and **5)** on cell-cycle progression in *L. donovani*. Treatment resulted in an accumulation of cells in G1 and in G2/M and a decrease in the proportion of cells in S phase (see **Fig 3a** for data for **5**), suggesting blocks in the cell-cycle at G1/S and G2/M. These results are consistent with a mode of action via CRK and/or CYC components.

Resistance was generated in *L. donovani* promastigotes *in vitro* against compounds **4** and **7**, with individual clones showing > 500-fold and 9- to 17-fold resistance, respectively (Extended Data Table 6). Resistance to both compounds was found to be stable over 50 days in culture in the absence of drug pressure and, significantly, all clones showed cross-resistance to **4** and **7**, and 20– and 50-fold cross-resistance to **5**. These data suggest our pyrazolopyrimidines share common mechanisms of resistance and therefore modes of action. Importantly, intracellular amastigotes, derived from the resistant promastigotes, were 8.5-fold and 5-fold resistant to **7** and **5**, respectively, compared to wild-type parasites (Extended Data Table S7). These data strongly suggest that the mechanism of action of these compounds is the same in promastigote and intracellular amastigote stages of the parasite.

To gain further insight into the mechanism of action and potential target(s) of this pyrazolopyrimidine series, we undertook a whole genome sequencing approach. Three clones independently selected for resistance to compound **4** and three clones independently selected for resistance to compound **7** were used to identify new mutations relative to parental, passaged-control clones (Table S5). A range of mutations were found across the genome (Table S5),

including a long region with loss of heterozygosity on chromosome 9. In total, 75 sites were identified genome-wide that each had single base substitutions resulting in a non-synonymous change in at least one clone (Table S6). The majority (65) of non-synonymous substitutions consisted of derived clones losing a parental allele but amplifying the remaining allele. In five of the six resistant clones a new heterozygous substitution was selected in a single gene of unknown function (LdBPK_251630) but most strikingly, in all 6 drug-resistant clones, a single homozygous non-synonymous substitution was found in CRK12 (LdBPK_090270), a gene within the long loss-of-heterozygosity region. This mutation changes Gly572 to Asp and falls within the region predicted to encode the catalytic domain of *L. donovani* CRK12. This suggests that CRK12 is the target of the pyrazolopyrimdines. Extensive variations in chromosomal copy numbers are common in *Leishmania*[23,24], and extra copies of chromosome 9, which contains the *CRK12* gene, were found in four out of six drug-resistant clones (Table S7). Additionally, three of these four clones had extra copies of chromosome 32, which contains the gene for CYC9. Previous studies in *T. brucei* have established that the partner cyclin of CRK12 is CYC9[25]. Taken together, these data suggest that CYC9 may be the cognate cyclin partner for *L. donovani* CRK12. Further CYC9 was identified alongside CRK12 in almost all chemical proteomics studies (*vide infra*).

Target validation

To dissect the role of CRK12 and CYC9 in the mechanism of action and resistance of pyrazolopyrimidines a series of protein overexpression studies were undertaken in *L. donovani* promastigotes. In all cases, overexpression of putative targets was confirmed by elevated levels of transcripts in our transgenic cell lines relative to WT, as determined by qRT-PCR (Table S8).

Counter-intuitively, overexpression of wild-type CRK12 ($CRK12^{WT}$) rendered the parasites ~3-fold *more* sensitive to **7**. The overexpression of CYC9 alone had no effect on compound resistance, but co-overexpression of CYC9 and $CRK12^{WT}$ rendered the transgenic parasites ~3-fold resistant to compounds **5** and **7** (Fig. 3c). Next, we looked at the mutated (Gly572 to Asp) version of CRK12 ($CRK12^{MUT}$) identified in all 6 of our drug-resistant clones. As expected, overexpression of $CRK12^{MUT}$ rendered the parasites ~3.4-fold resistant to **7** (Fig. 3b and Table S8) and to the pre-clinical lead compound **5**, while being equally sensitive to the unrelated nitroimidazole drug fexinidazole sulfone (Table S4). Co-overexpression of $CRK12^{MUT}$ and CYC9 rendered the parasites ~6-fold resistant to compound **5** and ~8-fold resistant to compound **7.** This shift in sensitivity is considerably greater than the 3.4-fold resistance observed with parasites overexpressing $CRK12^{MUT}$ alone (Fig. 3b).

Initially, CRK3 and CRK6 were identified as credible targets based upon our collective proteomics datasets, as well as their established roles in kinetoplastid cell cycle regulation[26,27]. However, whole genome sequencing, qPCR (Fig. S8) and Southern blot (Fig. S7) analysis of resistant clones confirmed that mutations within, or amplification of, the CRK3 and CRK6 genes were not responsible for resistance to pyrazolopyrimidines. Direct modulation of CRK3 and CRK6 levels within *L. donovani* promastigotes, by generating overexpressing and single gene knockout parasites, did not alter drug sensitivity (Table S8). Overexpression of CRK3 and CRK6 in combination with their cognate cyclin partners CYC6 and CYC3 was not possible since co-overexpression proved toxic. Collectively, these data suggest that the primary mechanism of action of this compound series is unlikely to be via CRK3 or CRK6 inhibition.

Commonly, overexpression of a compound's molecular target is accompanied by an increase in drug resistance. With this in mind, our collective data strongly suggest that the principal

target of our pyrazolopyrimidine series is the CYC9-activated form of CRK12, such that overexpression of CRK12 and CYC9 together provides resistance. This hypothesis is also consistent with the amplification of both *CRK12* and *CYC9* genes in resistant parasites; as well as the identification of both proteins in our SILAC and kinobead^{TM} proteomic datasets. That overexpression of CYC9 alone has no effect suggests that CYC9 is, to some extent, in excess over CRK12 and thus overexpression of CRK12^{MUT} can provide (~3-fold) resistance that is increased when additional CYC9 is co-expressed (~8-fold). The "hyper-sensitivity" of parasites overexpressing CRK12^{WT} alone to these compounds remains perplexing. One potential explanation is that CRK12^{WT} bound to a pyrazolopyrimidine in the absence of a CYC9 subunit is particularly toxic to the parasite. Alternatively, elevated levels of CRK12 may well sequester other cyclins thereby preventing their essential interactions with other CRKs. Further studies will be required to test these hypotheses.

Given that the compounds from this chemical series were found to interact with protein kinases, in particular CRK12, we used Cellzome's Kinobead^{TM} technology[13,28,29] with *L. donovani* axenic amastigote extracts to identify pyrazolopyrimidine-binders in the *Leishmania* kinome. These experiments were performed in the presence or absence of an excess of the soluble parent compound **7**. All proteins captured by the beads were quantified by TMT tagging of tryptic peptides followed by LC-MS/MS analysis[30]. CRK12, MPK9, CRK6 and CYC3 were identified, consistent with the other experiments above. A dose response experiment was performed in which **7** was added over a range of concentrations in order to establish a competition-binding curve and determine a half-maximal inhibition (IC_{50}) value (**Fig. 4b**). The IC_{50} values obtained in these experiments represent a measure of target affinity, but are also affected by the affinity of the target for the bead-immobilized ligands. The latter effect can be deduced by determining the depletion

of the target proteins by the beads, such that apparent dissociation constants (K_d^{app}) can be determined which are largely independent from the bead ligand[30]. The apparent dissociation constants (K_d^{app}) were determined to be 1.4 nM for CRK12, 45 nM for MAPK9, 58 nM for CYC3 and 97 nM for CRK6. These values are determined in physiological conditions and provides further compelling evidence that the principal target of this compound series is CRK12. Further pull-downs with a resin-bound pyrazolopyrimidine analogue (**11**) were conducted in parallel with the Kinobead™ experiments and returned broadly similar results (**Fig 4 c, d**)

Modelling

A homology model was built for *L. donovani* CRK12 using the structure of human cyclin dependent kinase 9 (CDK9, PDB code:4BCF) as a template. (Interestingly **5** showed an IC_{50} > 20 μM against CDK9 in the Kinobeads™ assay.) A combination of docking studies, molecular dynamics simulation and free energy calculations indicated the most likely binding mode is that shown in Figure 5 (see supporting information for discussion). With very few exceptions, the binding modes of protein kinase inhibitors are highly conserved across kinase family members; searching the protein database revealed a related 5-amino pyrazolopyrimidine, which bound to ALK in a very similar fashion (PDB code 4Z55, ligand 4LO). In our proposed binding mode, the bicyclic scaffold interacts with the hinge residues establishing two hydrogen bond between the sp^2 pyrimidine nitrogen in position 6 and the backbone NH of Ala564 and between the pyrazole NH in position 1 and the backbone carbonyl oxygen of Ala562 (Fig. 5b). A third hydrogen bond is also established between the amino NH in position 5 and the backbone carbonyl oxygen of Ala564. The substituent in position 3 of the pyrazole ring is directed towards the ATP back pocket interfacing with the gatekeeper residue Phe561. This binding mode is consistent with the PEG-linked analogues **10** and **11** retaining activity, with the PEG linkers being attached to water-

accessible parts of the core. The Gly572Asp mutation causing resistance to the pyrazolopyrimidine series is located at the end of the hinge region nine residues from the gatekeeper (Phe563). In the Gly572Asp mutant, the negatively charge side chain of the aspartic acid is positioned in close contact to the two sp^2 oxygen atoms of the sulphonamide moiety leading to an unfavorable electrostatic interaction.

Discussion

Our studies indicate that the principal mechanism of action of our pyrazolopyrimidine compounds is through inhibition of CRK12, defining CRK12 as one of very few chemically-validated drug targets in *Leishmania*. Further, our data indicate that CYC9 is the definitive partner cyclin for CRK12. The physiological function(s) of CRK12/CYC9 have yet to be determined and the availability of our inhibitory pyrazolopyrimidines should assist in probing this aspect of parasite biology.

It is clear from our collective chemical proteomics studies that the pyrazolopyrimidines also interact with other *Leishmania* protein kinases, in particular CRK6 and CRK3, albeit with significantly lower affinities than for CRK12. While CRK12 is undoubtedly the principal target of this compound series, we cannot rule out the possibility that underlying this mechanism of action is an element of polypharmacology. Indeed, inhibition of secondary kinase targets may be responsible for some of the phenotypic effects we observe in drug-treated parasites, such as cell cycle arrest.

In summary, we have identified a drug-like, anti-leishmanial compound series with clinical level efficacy in a VL mouse model of infection, which acts by an entirely novel mechanism of action (principally inhibition of CRK12). The compound **DDD853651 / GSK3186899** (compound

5) is being advanced towards human clinical trials and is currently undergoing preclinical development.

End notes

Supplementary Information: this contains chemical synthesis and characterization, methodology and ethical statements.

Acknowledgments: The authors acknowledge the Wellcome Trust for funding (grants, 092340, 105021, 100476, 101842, 079838, 098051).

Author Contributions: these are recorded in the supporting information

Author Information: Reprints and permissions information is available at www.nature.com/reprints. The authors declare the following financial interests: these authors have shares in GlaxoSmithKline. Correspondance and requests for materials should be addressed to Ian Gilbert (i.h.gilbert@dundee.ac.uk), Kevin Read (k.read@dundee.ac.uk) or Tim Miles (tim.j.miles@gsk.com).

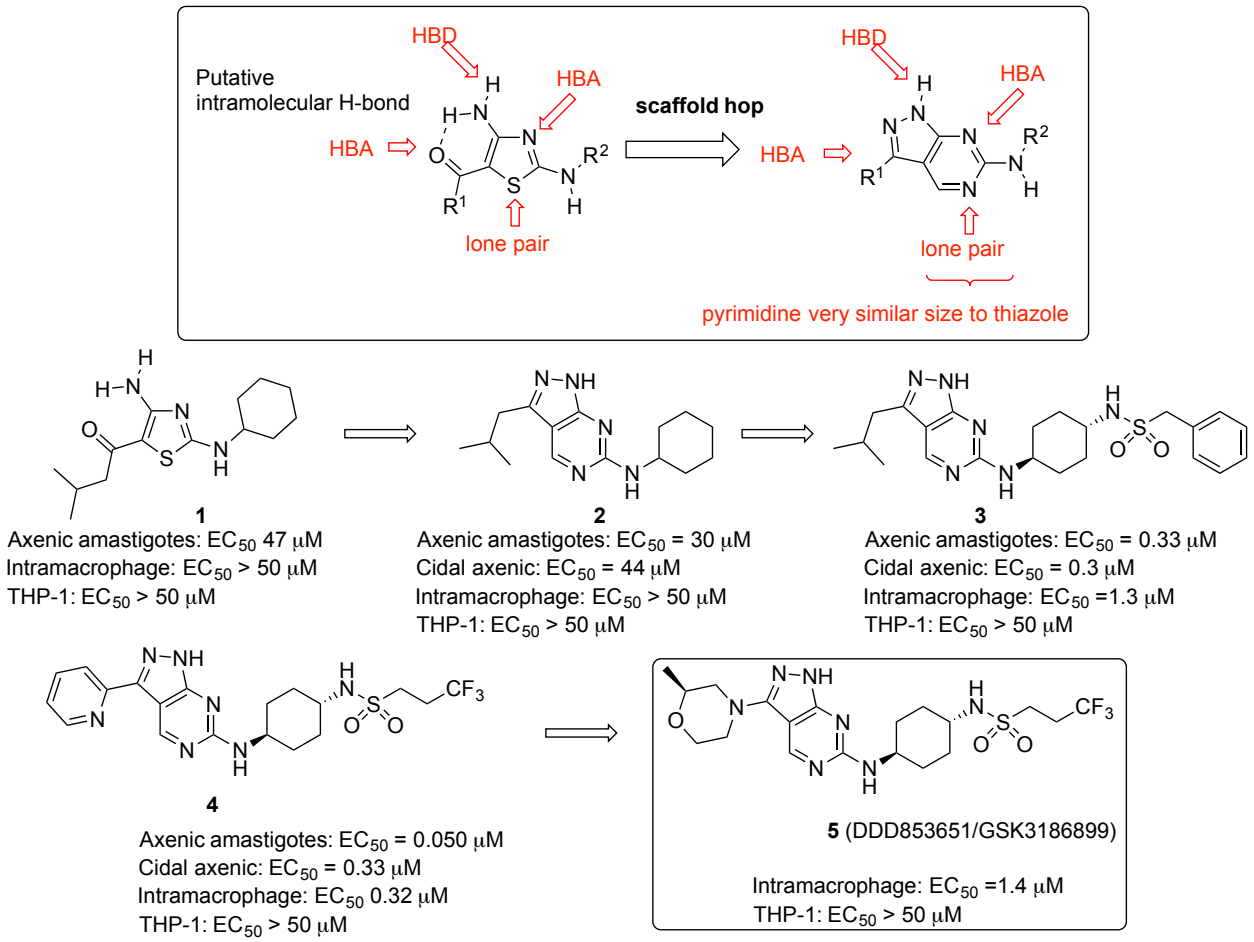

Figure 1: The evolution of the pyrazolopyrimidine series to give the development compound **5**. The potencies against axenic amastigotes, intramacrophage amastigotes and against THP-1 cells are shown[8]; data from ≥ 3 independent replicates for cidal axenic and intramacrophage assays.

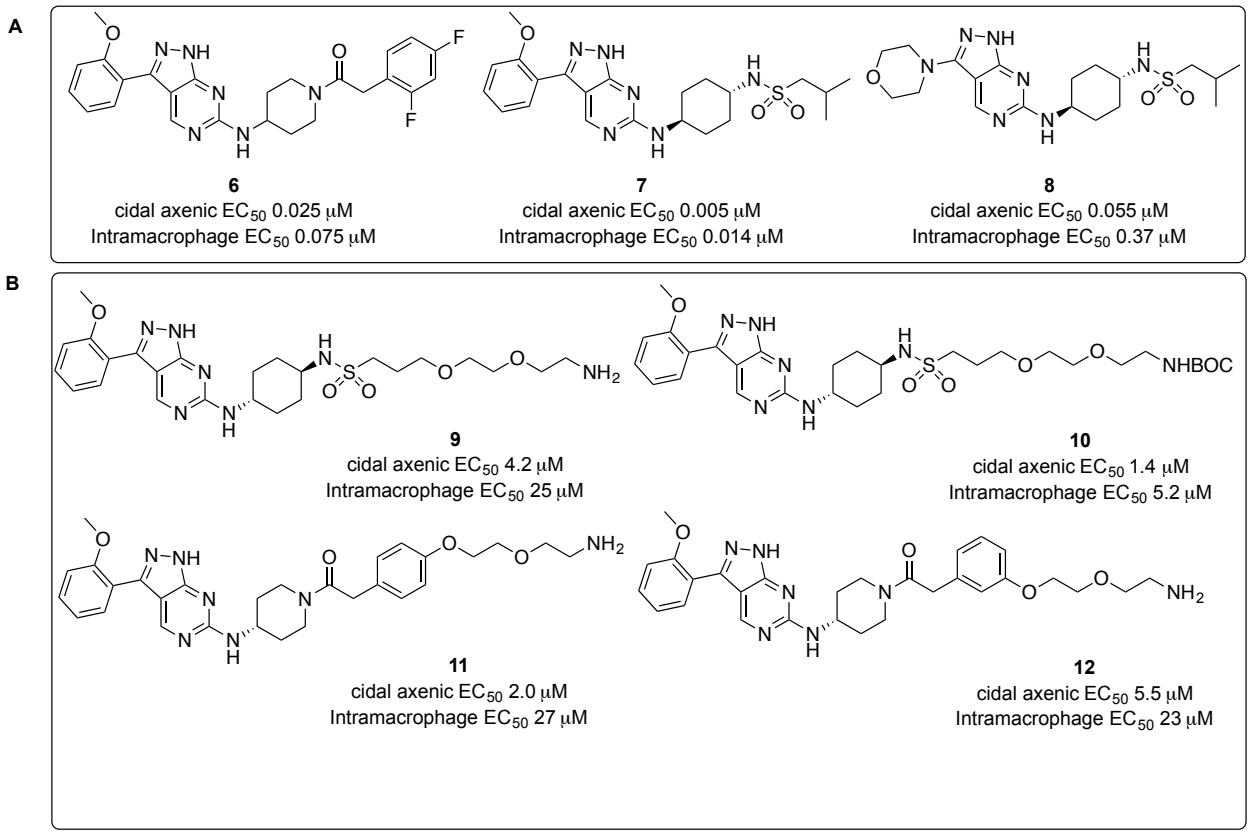

Figure 2 a) Additional compounds from the pyrazolopyrimidine series used for mode of action studies. **b)** Linker-containing pyrazolopyrimidine analogues prepared for mode of action studies. Activities in the cidal axenic[10] and intramacrophage assays[8] are shown (data from ≥ 3 independent replicates).

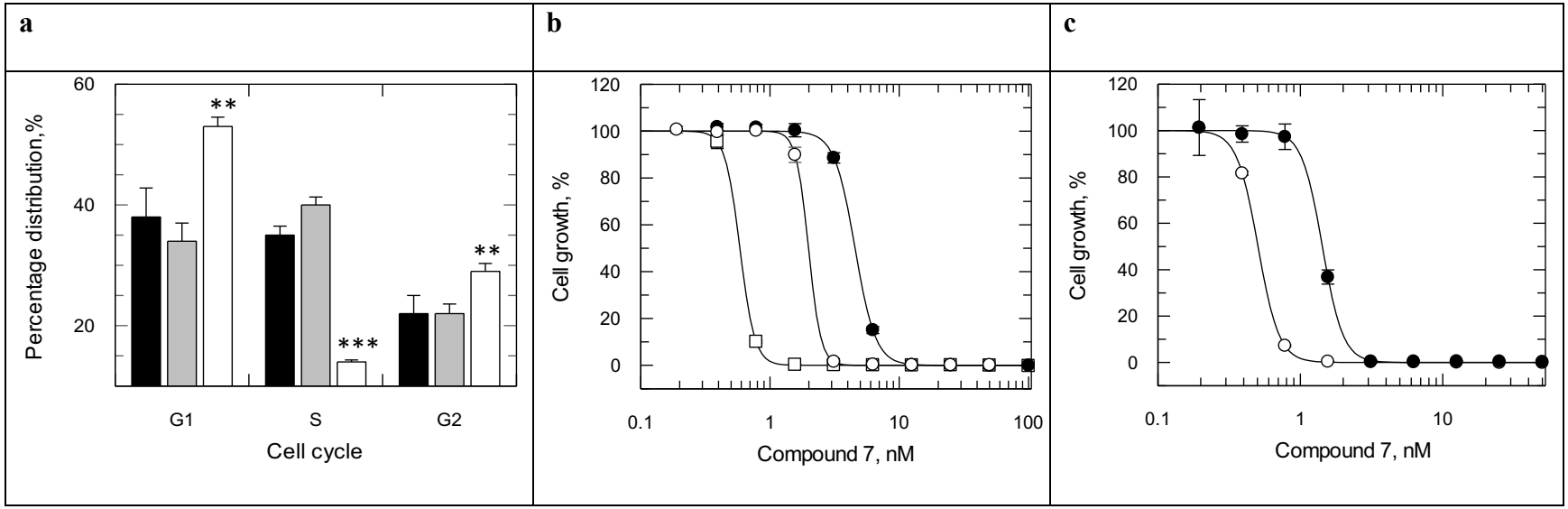

Figure 3: (a) Cell cycle analysis following treatment with compounds for 8 h. Untreated cells at 0 h (black) and at 8 h (grey). Cells treated with 5x EC_{50} value of compound **5** for 8 h (white). Differences in the percentage of drug-treated cells in the G1, S and G2 phases of the cell cycle were confirmed as statistically significant by using an unpaired Student t test (**, P = 0.01; ***, P = 0.001). **(b)** Effects of $CRK12^{MUT}$ and CYC9 overexpression on the potency of compound **7**. Susceptibility to compound **7** is decreased in $CRK12^{MUT}$-overexpressing promastigotes (EC_{50} value of 1.99 ± 0.002 nM, open circles) compared to WT cells (EC_{50} value of 0.59 ± 0.001 nM open squares) and further decreased in $CRK12^{MUT}$/CYC9 co-overexpressing promastigotes (EC_{50} value of 4.6 ± 0.05 nM, closed circles). **(c)** Effects of $CRK12^{WT}$ and CYC9 co-overexpression on the potency of compound **7**. Susceptibility to compound **7** is decreased in

promastigotes overexpressing CRK12^{WT} and CYC9 (EC_{50} value of 1.43 ± 0.01 nM, closed circles) compared to WT cells (EC_{50} value of 0.5 ± 0.004 nM, open circles). All data are the mean ± SD of triplicate cultures from at least a single experiment.

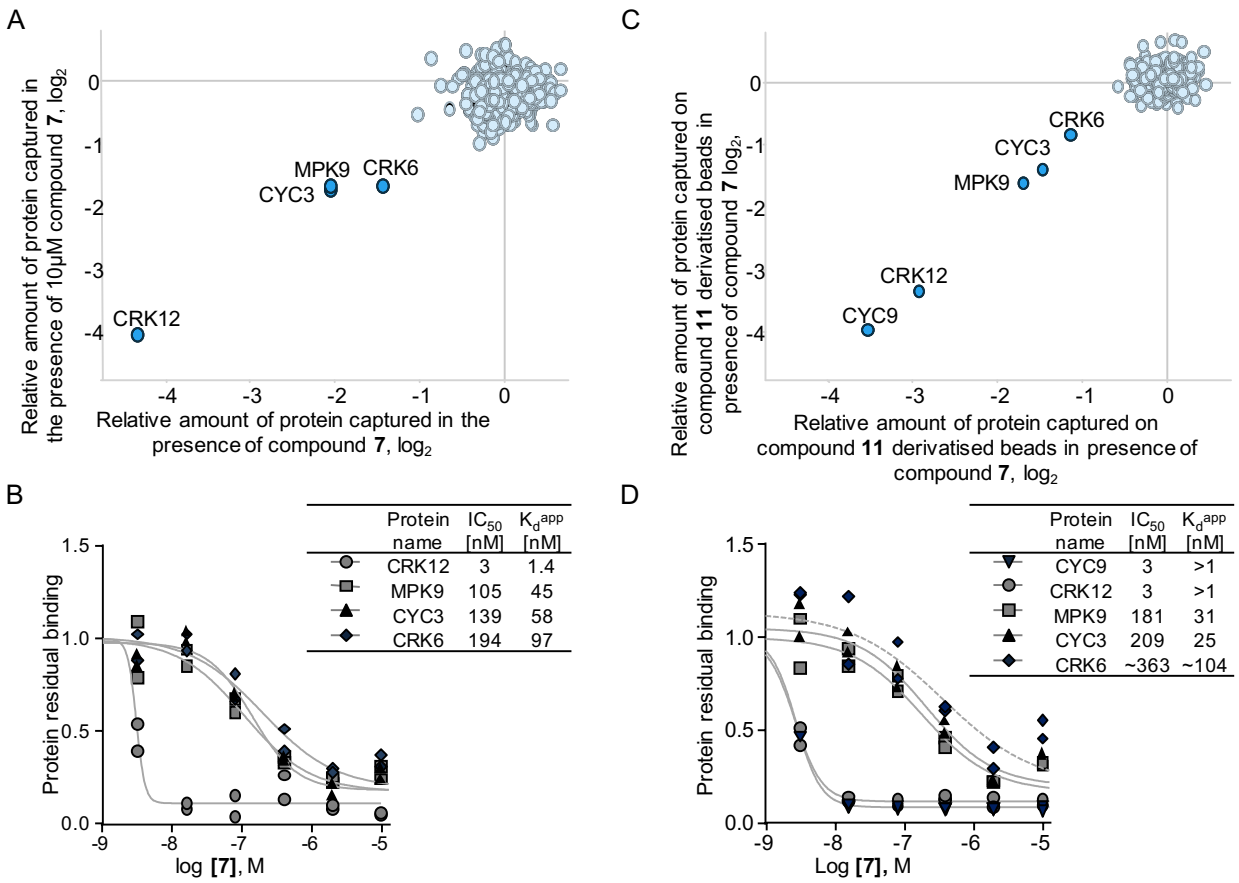

Figure 4. Identification of cyclin dependent related kinases as targets of the pyrazolopyrimidine series using a chemoproteomic approach. a) Relative amounts of protein captured on Kinobeads™ in the presence of 10 µM compound **7** compared to vehicle, compared in 2 experiments. A $\log_2$ scale is used. **b)** Dose response curves of binding of CRK12, MPK9, CYC3 and CRK6 to Kinobeads™ in the presence of varying concentrations of compound **7**. **c)** Relative amounts of protein captured on **11** in the presence of 10 µM compound **7** compared to vehicle, compared in 2 experiments. A $\log_2$ scale is used. **d)** Dose response curves of binding of CYC9, CRK12, MPK9, CYC3 and CRK6 to **11**-derivatised beads in the presence of varying concentrations of **7**.

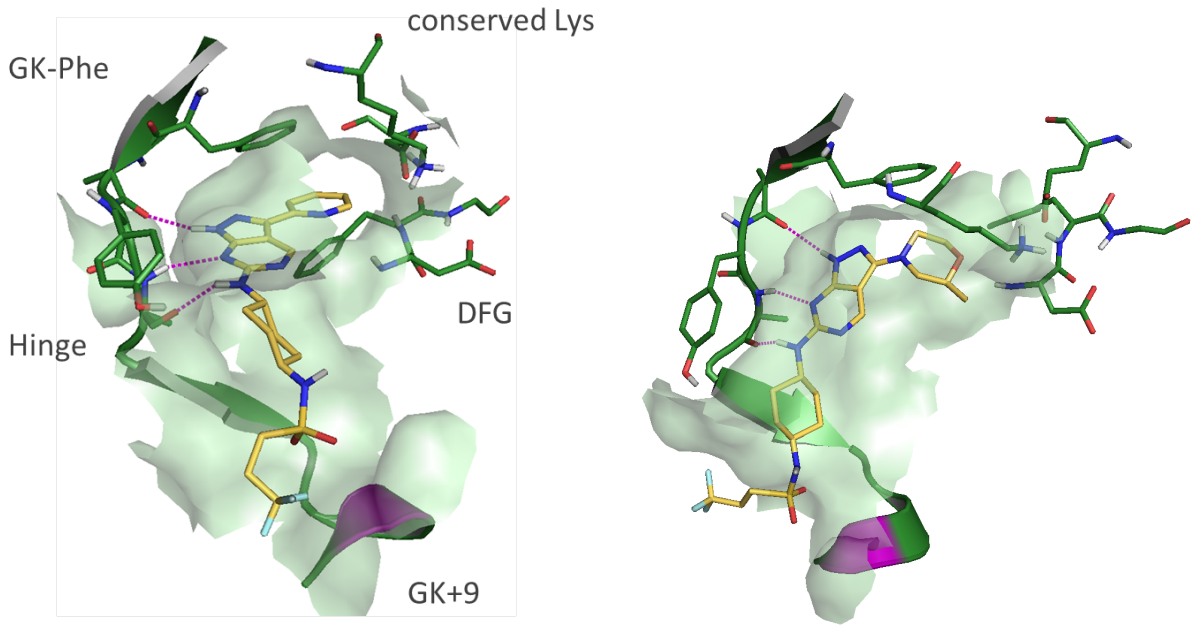

Figure 5. Docking poses for **a) 4** and **b) 5.** Dotted purple lines represent H-bonds. The mutated residue in position Gate-Keeper + 9 is indicated in purple in the ribbon diagram.

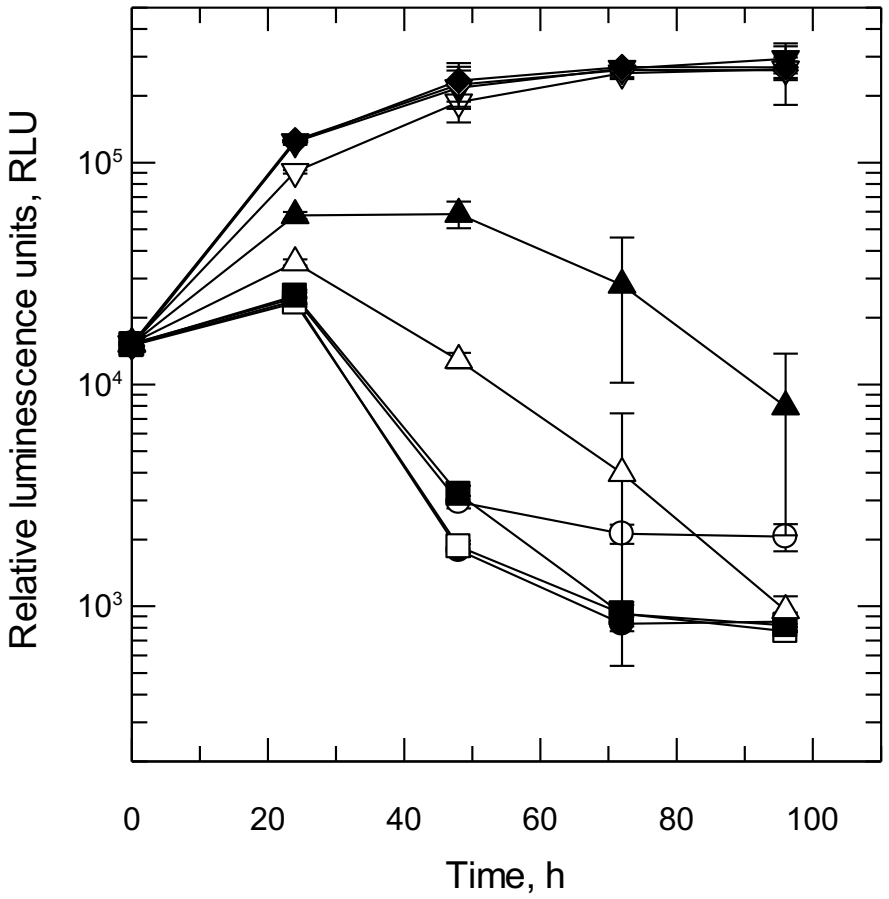

Extended Data Figure 1: Rate-of-kill of *L. donovani* axenic amastigotes by compound **5**. Chart shows relative luminescence units (RLU) versus time from axenic amastigote rate-of-kill experiment with compound **5** (n = 3, error bars = standard deviation). Concentrations are as follows (μM): 50, open circles; 16.7, closed circles; 5.6, open squares; 1.85, closed squares; 0.62, open triangles; 0.21, closed triangles; 0.069, open inverted triangles; 0.023, closed inverted triangles, 0.0076, open diamond and 0.0025, closed diamond.

Extended Data Table 1. Activity of compound 5 and miltefosine against a panel of *Leishmania* clinical isolates (intra macrophage assay using human peripheral blood mononuclear cells)

Strain	Country of origin	Year	Compound **5** EC_{50} (μM)	Miltefosine EC_{50} (μM)
L. donovani LV9	Ethiopia	1967	0.06	0.40
L. donovani SUKA 001	Sudan	2010	0.10	1.0
L. donovani BHU1 *	India	2002	0.10	0.50
L. donovani DD8	India	1980	0.13	0.50
L. infantum ITMAP263	Morocco	1967	0.13, 0.50	0.79

* Antimony-resistant reference strain

Strains were tested on a single (DD8, SUKA001, BHU1) or two (LV9, ITMAP263) test occasions; for ITMAP263 the respective EC_{50} values are shown.

Extended Data Table 2. Solubility of compound 5 in simulated physiological media (4h at 37°C).

Media	Final pH	Solubility [mg/mL]
SGF pH1.6	SGF (1.5)	1.12
Fasted SIF pH6.5	FaSSIF (6.5)	0.017
Fed SIF pH6.5	FeSSIF (6.5)	0.025

SGF, Simulated Gastric Fluid; SIF, Simulated Intestinal Fluid. Data for polyform 1.

Extended Data Table 3. *In vitro* metabolic stability data for compound 5.

Species	Concentration (μM)	Microsomes Cli (mL/min/g tissue)	Hepatocytes Cli (mL/min/g tissue)
Mouse	0.5	0.52	0.84
Rat	0.5	<0.5	0.77
Dog	0.5	<0.4	0.31
Human	0.5	0.71	0.5

Extended Data Table 4. DMPK data for compound 5

	Mouse (male, CD1)	Rat (male, SD)
Intravenous	1 mg/kg	1 mg/kg
Cl (ml/min/kg)	169 ± 50	14 ± 9
Vdss (L/kg)	4.0 ± 0.5	0.4 ± 0.2
$T_{1/2}$ (h)	0.3 ± 0.04	0.4 ± 0.1
$AUC_{(0\text{-inf})}$ (ng.h/mL)	104 ± 26	1514 ± 782
Oral	10 mg/kg	10 mg/kg
Cmax (ng/ml)	561 ± 148	1043 ± 261
T_{max} (h)	2	2
$T_{1/2}$ (h)	1.2 ± 0.4	2.5 ± 0.6
$AUC_{(0\text{-inf})}$ (ng.h/mL)	1463 ± 362	6475 ± 2494
F% based on $AUC_{(0\text{-inf})}$	>100	46 ±18
Oral	100 mg/kg	100 mg/kg
Cmax (ng/ml)	8813 ± 1966	8470 ± 3750
Tmax (h)	3	7.3
$T_{1/2}$ (h)	2.6 ± 0.8	2.1 ± 0.1
$AUC_{(0\text{-inf})}$ (ng.h/mL)	39433 ± 23830	61202 ± 23591
F% based on $AUC_{(0\text{-inf})}$	>100	40 ± 15
Oral	300 mg/kg	300 mg/kg
Cmax (ng/ml)	11393 ± 4212	14833 ± 2676
Tmax (h)	5	7.3
$T_{1/2}$ (h)	2.5 ± 0.6	2.8 ± 0.6
$AUC_{(0\text{-inf})}$ (ng.h/mL)	66150 ± 636	136333 ± 24846
F% based on $AUC_{(0\text{-inf})}$	>100	51 ± 22

Extended Data Table 5: Efficacy data for compound 5

Dose (mg/kg)	Frequency	Duration (days)	Reduction in parasite load (%)
50	bid	5	96
25	bid	10	99
10	bid	10	49
3	bid	10	4
50	uid	5	50
25	uid	10	89
50	uid	10	95

The $ED_{50,}$ ED_{90} and ED_{99} values for compound **5** following 10 day treatment orally b.i.d. are 10.1 mg/kg, 17.4 mg/kg and 31.5 mg/kg, respectively. The reported ED_{90} for miltefosine in a mouse model is 27 mg/kg u.i.d. [31,326]

Extended Data Table 6. Sensitivity of WT and drug-resistant promastigotes to compounds within the series. Resistance was generated against compounds 4 and 7.

Cell line	4		7		5	
	pEC_{50} (SD)	Fold	pEC_{50} (SD)	Fold	pEC_{50} (SD)	Fold
Wild type (Start clone)	7 (0.1)	1	8.2 (0.4)	1	7.1 (0.3)	1
Wild type (Age-matched)	7.1 (0.2)	1	8.2 (0.1)	1	7.3 (0.2)	1
4-resistant clone 1	< 4.3	>500	7.2 (0.1)	11	5.8 (0.4)	20
4-resistant clone 2	< 4.3	>500	7.3 (0.1)	7	5.7 (0.2)	24
4-resistant clone 3	< 4.3	>500	7 (0.2)	17	5.4 (0.1)	48
7-resistant clone 1	< 4.3	>500	7.1 (0.2)	11	5.5 (0.2)	41
7-resistant clone 2	< 4.3	>500	7.1 (0.2)	14	5.5 (0.1)	35
7-resistant clone 3	< 4.3	>500	7.3 (0.1)	9	5.7 (0.1)	22

Extended Data Table 7: Sensitivity of WT and compound 7-resistant intracellular amastigotes (INMAC) to the compound series.

Compound	Cell line	pXC50	Host cell pXC_{50}	Fold difference
7	WT	7.5	<5.3	-
7	**7** RES clone 1	6.6	<5.3	8.5
5	WT	5.9	<4.3	-
5	**7** RES clone 1	5.2	<4.3	5.0

1 Alvar, J. *et al.* Leishmaniasis worldwide and global estimates of its incidence. *PLoS One* **7**, e35671, (2012).
2 Ritmeijer, K. & Davidson, R. N. Royal Society of Tropical Medicine and Hygiene joint meeting with Medecins Sans Frontieres at Manson House, London, 20 March 2003: field research in humanitarian medical programmes. Medecins Sans Frontieres interventions against kala-azar in the Sudan, 1989-2003. *Trans R Soc Trop Med Hyg* **97**, 609-613, (2003).
3 Sundar, S. *et al.* Efficacy of miltefosine in the treatment of visceral leishmaniasis in India after a decade of use. *Clin Infect Dis* **55**, 543-550, (2012).
4 den Boer, M. L., Alvar, J., Davidson, R. N., Ritmeijer, K. & Balasegaram, M. Developments in the treatment of visceral leishmaniasis. *Expert opinion on emerging drugs* **14**, 395-410, (2009).
5 Mueller, M. *et al.* Unresponsiveness to AmBisome in some Sudanese patients with kala-azar. *Trans R Soc Trop Med Hyg* **101**, 19-24, (2007).
6 Don, R. & Ioset, J.-R. Screening strategies to identify new chemical diversity for drug development to treat kinetoplastid infections. *Parasitology* **141**, 140-146, (2014).
7 Woodland, A. *et al.* From on-target to off-target activity: identification and optimisation of *Trypanosoma brucei* GSK3 inhibitors and their characterisation as anti-*Trypanosoma brucei* drug discovery lead molecules. *ChemMedChem* **8**, 1127-1137, (2013).
8 De Rycker, M. *et al.* Comparison of a high-throughput high-content intracellular *Leishmania donovani* assay with an axenic amastigote assay. *Antimicrob Agents Chemother* **57**, 2913-2922, (2013).
9 Miles, T. J. & Thomas, M. G. Pyrazolo[3,4-d]pyrimidin derivative and its use for the treatment of leishmaniasis WO 2016116563 A1 20160728 (2016).
10 Nuhs, A. *et al.* Development and Validation of a Novel Leishmania donovani Screening Cascade for High-Throughput Screening Using a Novel Axenic Assay with High Predictivity of Leishmanicidal Intracellular Activity. *PLoS Negl Trop Dis* **9**, e0004094, (2015).
11 Ding, Q., Jiang, N. & Roberts, J. L. Preparation of pyrazolopyrimidines as antitumor agents. WO 2005121107 (2005).
12 Ding, Q., Jiang, N. & Roberts, J. L. Preparation of pyrazolopyrimidines as antitumor agents. US 20050277655 (2005).
13 Bantscheff, M. *et al.* Quantitative chemical proteomics reveals mechanisms of action of clinical ABL kinase inhibitors. *Nat. Biotechnol.* **25**, 1035-1044, (2007).
14 Terstappen, G. C., Schlupen, C., Raggiaschi, R. & Gaviraghi, G. Target deconvolution strategies in drug discovery. *Nat Rev Drug Discov* **6**, 891-903, (2007).
15 Park, J., Koh, M. & Park, S. B. From noncovalent to covalent bonds: a paradigm shift in target protein identification. *Mol Biosyst* **9**, 544-550, (2013).
16 Lee, H. & Lee, J. W. Target identification for biologically active small molecules using chemical biology approaches. *Archives of pharmacal research*, (2016).
17 Ursu, A. & Waldmann, H. Hide and seek: Identification and confirmation of small molecule protein targets. *Bioorg Med Chem Lett* **25**, 3079-3086, (2015).
18 Urbaniak, M. D., Guther, M. L. S. & Ferguson, M. A. J. Comparative SILAC Proteomic Analysis of Trypanosoma brucei Bloodstream and Procyclic Lifecycle Stages. *PLoS One* **7**, e36619, (2012).
19 Liu, Y. & Gray, N. S. Rational design of inhibitors that bind to inactive kinase conformations. *Nat Chem Biol* **2**, 358-364, (2006).
20 Zhang, L. *et al.* Design, synthesis, and biological evaluation of pyrazolopyrimidine-sulfonamides as potent multiple-mitotic kinase (MMK) inhibitors (part I). *Bioorg Med Chem Lett* **21**, 5633-5637, (2011).
21 Freyne, E. J. E. *et al.* Pyrazolopyrimidines as cell WO2006074984 (2006).
22 Bengs, F., Scholz, A., Kuhn, D. & Wiese, M. LmxMPK9, a mitogen-activated protein kinase homologue affects flagellar length in Leishmania mexicana. *Mol Microbiol* **55**, 1606-1615, (2005).
23 Rogers, M. B. *et al.* Chromosome and gene copy number variation allow major structural change between species and strains of Leishmania. *Genome Res* **21**, 2129-2142, (2011).
24 Downing, T. *et al.* Whole genome sequencing of multiple Leishmania donovani clinical isolates provides insights into population structure and mechanisms of drug resistance. *Genome Res* **21**, 2143-2156, (2011).

25 Monnerat, S. *et al.* Identification and Functional Characterisation of CRK12:CYC9, a Novel Cyclin-Dependent Kinase (CDK)-Cyclin Complex in. *PLoS One* **8**, e67327, (2013).
26 Hassan, P., Fergusson, D., Grant, K. M. & Mottram, J. C. The CRK3 protein kinase is essential for cell cycle progression of Leishmania Mexicana. *Molecular and Biochemical Parasitology* **113**, 189-198, (2001).
27 Tu, X. & Wang, C. C. Pairwise knockdowns of cdc2-related kinases (CRKs) in Trypanosoma brucei identified the CRKs for G1/S and G2/M transitions and demonstrated distinctive cytokinetic regulations between two developmental stages of the organism. *Eukaryot. Cell* **4**, 755-764, (2005).
28 Medard, G. *et al.* Optimized chemical proteomics assay for kinase inhibitor profiling. *J Proteome Res* **14**, 1574-1586, (2015).
29 Bergamini, G. *et al.* A selective inhibitor reveals PI3Kgamma dependence of T(H)17 cell differentiation. *Nat Chem Biol* **8**, 576-582, (2012).
30 Bantscheff, M. *et al.* Chemoproteomics profiling of HDAC inhibitors reveals selective targeting of HDAC complexes. *Nat Biotechnol* **29**, 255-265, (2011).
31 Seifert, K. & Croft, S. L. In vitro and in vivo interactions between miltefosine and other anti-leishmanial drugs. *Antimicrob. Agents Chemother.* **50**, 73-79, (2006).
32 Escobar, P., Yardley, V. & Croft, S. L. Activities of hexadecylphosphocholine (miltefosine), AmBisome, and sodium stibogluconate (Pentostam) against Leishmania donovani in immunodeficient scid mice. *Antimicrob Agents Chemother* **45**, 1872-1875, (2001).